

LiM 2011

# Crack Free Tungsten Carbide Reinforced Ni(Cr) Layers obtained by Laser Cladding

J. M. Amado<sup>a</sup>, M. J. Tobar<sup>a</sup>, A. Yáñez<sup>a\*</sup>, V. Amigó<sup>b</sup>, J. J. Candel<sup>b</sup>

<sup>a</sup>Universidad de Coruña, Campus de Esteiro s/n, 15403, Ferro

<sup>b</sup>ITM-UPV, c/ Vera s/n, 46022 Valencia

---

## Abstract

The development of hardfacing coatings has become technologically significant in many industries. A common approach is the production of metal matrix composites (MMC) layers. In this work NiCr-WC MMC hardfacing layers are deposited on C25 steel by means of laser cladding. Spheroidal fused tungsten carbides are used as reinforcement phase. Three different NiCr alloys with different Cr content were tested. Optimum conditions to obtain dense, uniform carbide distribution and hardness close to nominal values were defined. The effect of Cr content respect to the microstructure, susceptibility for cracking and the wear rate of the resulting coating will also be discussed.

*Keywords:* laser cladding; hardfacing; MMC; tungsten carbides; NiCr-WC

---

## 1. Introduction

Laser cladding [1] with metal matrix composites (MMC) may be used to deposit hardfacing coatings on metallic surfaces subjected to abrasive wear. MMCs consist of a mixture of hard, reinforcing phases immersed in a ductile metal matrix. The reinforcement constituent is normally a ceramic or a compound of a refractory metal as titanium, tungsten or chromium carbides. The matrix is usually a Ni or Co based alloy which further enhances the layer resistance to corrosion, particularly at high temperatures. This work studies the deposition of Ni based MMC layers on low carbon steel components by means of laser cladding. Tungsten carbides have been chosen as hard phase, given its high melting point, high hardness, low thermal expansion and good wettability by molten metals. Cladding with laser should further provide with more dense coatings, metallurgical bonding with substrates and minimal thermal distortion in the processed part as compared to other more standard deposition methods (thermal spraying, APS, ...).

In the present investigation three premixed NiCr-WC alloy powders are used, developed by the manufacturer, Technogenia, for coating applications with high power lasers. This company produces spheroidal fused tungsten carbides (commercialized under the name of Spherotene®) characterized by a extremely high hardness, quasi-monophasic composition (cubic non-stoichiometric  $W_{1-x}C$  fcc phase) and a very smooth finish. These carbide particles are used as reinforcing WC phases in the above referred alloys. The same type of spheroidal fused tungsten

---

\* Corresponding author. Tel.: +34-981-337400  
E-mail address: [ayanez@udc.es](mailto:ayanez@udc.es).

particles have already been used by other authors[2,3] at different concentrations and mixed with other types of Ni-based alloys.

The three premixed NiCr-WC alloys differ in the Cr content of the matrix. The aim of the study was to elucidate the effect of the matrix composition on the microstructure and wear performance of the obtained coatings.

## 2. Experimental

The laser cladding system consisted of a 2 kW industrial Nd-YAG laser (Rofin-Sinar DY22). Powder feeding is performed coaxially by means of a powder feeder (Sultzer-Metco Twin10c). Laser beam was defocused to a beam diameter of  $d=3.5$  mm on the working surface. Cladding was performed on 5 mm thick probes of low carbon steel C25 preheated to 400°C. Extend areas of approximately 30mmx 30mm were covered by overlapped laser scans, at 35%-40% overlapping ratios.

Table 1. Measured EDX composition of WC spheres and NiCr matrices.

WC	C	Fe	Ti	Ta	W		
Spherotene	3.8-3.9	<0.1	<0.05	<0.05	Bal.		
NiCr Matrix	C	Fe	Si	B	Cr	Co	Ni
Technolase 30	<0.6	2.6-3.4	3.4-3.9	1-1.3	6-8	<0.1	Bal.
Technolase 40	<0.6	2.5-3.5	2.5-3.6	1.3-2	8-11	<0.1	Bal.
Technolase 60	<0.6	4-4.5	3.5-4.5	2-3	12-14	<0.1	Bal.
Substrate	C	Mn	P	S	Si	Fe	
GS-C25	0.25	1.20	0.04	0.04	0.06	<1	Bal.

As noted at the introduction, three premixed NiCr-WC powder alloys, commercialized as Technolase60s, Technolase40s, Technolase30s (T60, T40 and T30 from here on), were employed for the laser cladding experiments. Both include Spherotene® as hard WC particles. Detailed chemical composition is given in Table 1. The nominal Cr content in the NiCr matrix is 12-14% wt., 8-11 % wt. and 6-8% wt. for T60, T40 and T30 respectively. In this order, data from the manufacturer assigns to each matrix a nominal hardness of 60HRC(700 HV), 40HRC(400HV) and 30HRC(300HV), which we address to the different Cr contents in the NiCr alloy. Tungsten carbide concentration is about +60% by weight in every case. Accounting for the different densities of the NiCr alloy particles and fused carbides, ~8 and ~16 gr/cm<sup>3</sup> respectively, around 40%-45% volume percentage of carbides is to be expected in the deposited coatings. Nominal Spherotene® carbide size is +40-160µm. Its nominal hardness range between 2500 and 3300 HV.

N<sub>2</sub> was used as the shielding and powder carrier gas. All samples were cut transversally, grounded, polished and etched. Cross-sections of resulting coatings were examined by optical and scanning electron microscopy (SEM), and their compositions were determined by energy dispersive X-ray (EDX) analysis. Microhardness measurements were performed. Liquid penetrant dye test was used to reveal cracks in the deposited layers.

Tests were performed on grounded coated surfaces for dry sliding wear using a microtest MT4002 tribometer with a pin-on-disk set up according with ASTM G99-05 standard for dry sliding wear. Al<sub>2</sub>O<sub>3</sub> balls of 4 mm diameter were used as counterbody. Their hardness is approximately 1500 HV. A sliding speed of 100 mms<sup>-1</sup> and normal load of 20 N was selected. The test was finished after a total distance of 500 m. After the test, the weight lost of the coating and counterbody were evaluated.

Table 2. Parameter phase space used in the study for NiCr-WC alloy deposition ( $d=3.5$  mm) on C25 low alloy steel.

$f/v$ (mg/mm)	$P/(vd)$ (J/mm <sup>2</sup> )	$v$ (mm/s)	$P$ (W)	$f$ (g/s)
25	[10-20]	10	350-700	0.25
		20	700-1400	0.50
		30	1100-2000	0.750
		40	1400-2000	1.00
35	[15-25]	10	550-900	0.35
		20	1100-1750	0.70
		30	1600-2000	1.00
40	[20-30]	10	700-1100	0.40
		20	1400-2000	0.8

### 3. Results and Discussion

#### 3.1. Morphology and Microstructure

Results on the morphology and microstructure of the deposited T60 and T40 coatings in terms of the laser cladding process parameters have already been published [4]. Varying the laser output power  $P$ [W], the scanning velocity  $v$ [mm/s] an powder mass flow rate  $f$ [gr/s], it was found that the specific energy density applied,  $P/(d.v)$ [J/s.mm<sup>2</sup>], should be as low as possible so as to have good quality MMC coatings and yet good bonding with the processed substrate. Otherwise, wide pores in the deposited material are obtained. This fact has been related to the excess energy causing high temperatures in the deposited alloy leading to the melting and dissolution of a significant proportion of the carbides. The decomposition of WC (producing free carbon) from the dissolution of tungsten carbide spheres gives rise to the porosity. It also leads to a significant presence of tungsten in the matrix, even with the formation of trapezoidal blocks rich in  $W_2C$  and WC phases, resulting in hardness values of the matrix of 1000-1400 HV, largely exceeding the nominal ones.

A parameter phase space for optimum cladding deposition was hence defined, as shown in Table 2. A total of 27 layers for each of the alloys were deposited corresponding to three different laser power values within pointed ranges for each of the feeding rates and scan speed conditions. Substrate preheating served to two objectives. Firstly, it helps to prevent cracking by reducing the cooling rates and diminishing thermal stresses effects. Secondly, it should be noted that in laser cladding part of the beam energy is absorbed by the powder material and the rest of the energy flux melts the substrate surface and lead to clad formation upon. If thermal conductivity of the metal substrate is high, as for low carbon steels, substantial power densities must be applied in order to effectively melt the metal surface. Besides, the melting point of C25 is significantly higher than that of the NiCr alloy (1530°C and 1038°C respectively). In summary, the projected clad material is subjected to an undesirable high energy irradiation. If substrate temperature is raised, its thermal conductivity is somewhat reduced, the laser absorption increases and the power needed for melt pool formation is significantly reduced. Therefore the cladding process can be performed with less energy absorption in the NiCr-WC alloy.

Table 3. Example of microhardness values obtained in T60, T40 and T30 layers.

	NiCr Matrix		WC sphere
	(HV <sub>0.2</sub> )		(HV <sub>0.2</sub> )
T60	934	884	2842
	884	896	
	596	570	
T40	535	518	2706
	475	450	
T30	468	481	3009

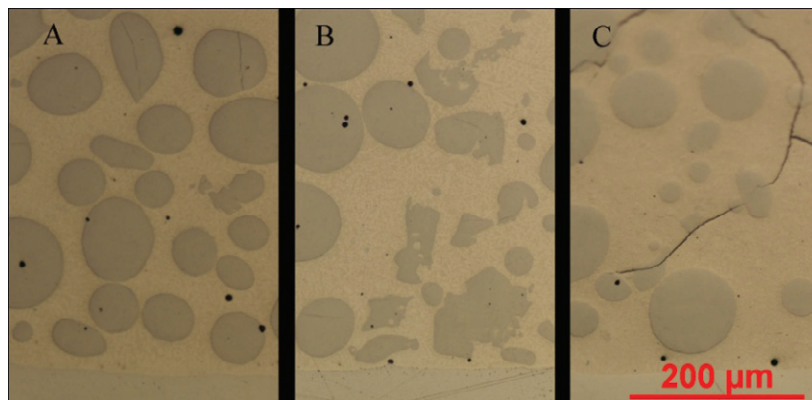


Figure 1. Optical micrograph of T30(A), T40(B) and T60(C) layers. Process parameters: 35 mg/mm, 20 mm/s, 1700 W.

As expected, pore free layers with good bonding with substrate and minimal dilution were obtained in all cases. Volume concentration of tungsten carbide spheres, as measured by image analysis, is close to the nominal 40% in all cases. This pattern was common to all samples processed in the defined parameter window. A magnified optical view of the layer microstructure can be seen in Fig 1, where the three different alloys are compared. The general appearance of the microstructure is equivalent for the three of them, showing carbide spheres embedded and uniformly distributed in the matrix. EDX measurements of the mean matrix composition gives values in agreement with the chemical composition of the NiCr alloys, yielding an increased content in Cr according to the alloy type. The Fe content, coming from dilution from the substrate, is minimal in all samples. Presence of W is found in all the analyzed specimens, which is addressed to dissolution of the smallest tungsten carbide spheres during the cladding process.

Fig. 2 show SEM micrographs of the samples, corresponding to T60, T40 and T30 layers. A good bonding of the reinforcement phase by diffusion in the matrix may be observed. The matrices conform to a dendritic solid solution of Ni with interdendritic eutectics. Additionally, one can notice the precipitation of mixed carbides (W,Cr)C all over the matrix. It was noticed as well that the size and amount of the precipitated carbides is larger for the T60

layers than those of T40 or T30. This may be due to the higher content of carbide former Cr in the first alloy type. In the coatings of T60, the interdendritic eutectic predominates over the nickel-phase dendrites and in the coatings of T30 nickel-phase dendrites are the predominant phase.

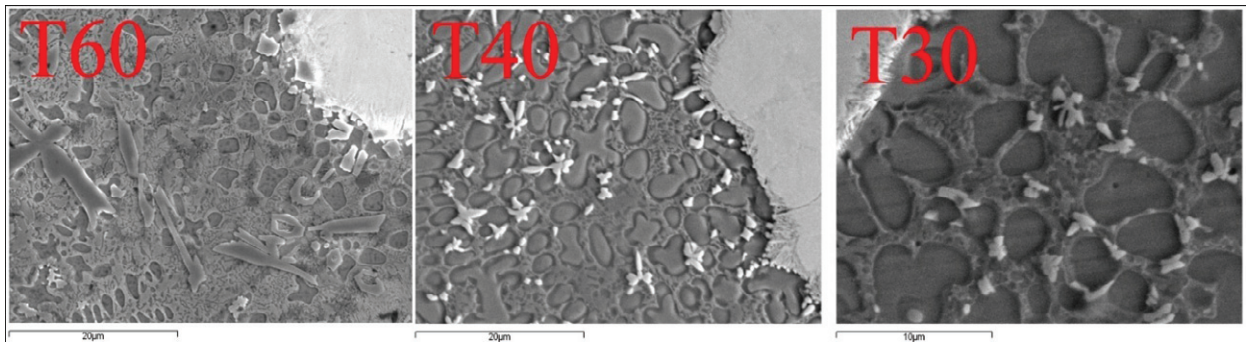


Figure 2. SEM micrograph showing the microstructure of a T60, T40 and T30 layers.

### 3.2. Microhardness

An example of the microhardness measurements corresponding to T60, T40 and T30 samples is listed in Table 3. In the table, values obtained at four different sites of the NiCr matrix are given. Carbide values correspond to a unique measurement in a carbide sphere. It is seen that matrix hardness is close to the nominal 700 HV, 400 HV and 300 HV values of the alloys NiCr matrix, indicating a minimized dissolution of the tungsten carbides. Carbide hardness also reproduce the  $3000 \pm 500$  HV value claimed by the manufacturer for this type of spheroidal tungsten carbides. The structure of the deposited coating therefore complies with the MMC requirements.

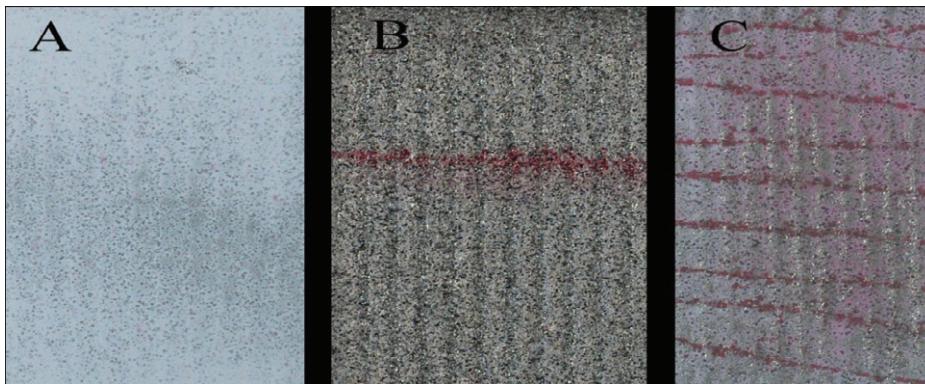


Figure 3. Results of liquid dye penetrant tests on T30(A), T40(B) and T60(C) layers.

### 3.2. Cracking susceptibility

Cracking could not be avoided in any of the processed samples of T60. A mean number of 10 cracks were observed along 40 mm length perpendicular to the laser scanning path, as seen in Fig 3. In Fig. 4 we can see two SEM images of a crack in the T60 layer. It was concluded that this cracking susceptibility is due to the own nature of the NiCr matrix. Nickel alloys with chromium, boron, and silicon contents represent a type of hardfacing alloys by means of the formation of nickel, chromium borides and complex carbides as dominant primary hard phases[5,6]. The hardness of these type of alloys, which can range up to 700HV(60HRC), increases with the precipitation of this hard phases which is mainly accomplished by increasing the Cr content of the alloy. However, these hard phases are

also very brittle, making the matrix alloy less ductile and more susceptible to the high thermal stress imposed by the high thermal gradients and solidification velocities associated to the laser cladding technique. In the coatings of T60, the interdendritic eutectic predominates over the nickel-phase dendrites and in the coatings of T30 nickel-phase dendrites are the predominant phase. The nickel-phase dendrites are very ductile. The fracture toughness (KIC) of nickel-base hardfacing alloys is accurately described by a crack-bridging model. Crack bridging in Ni-based alloys is described as “the toughening of the brittle matrix of carbide, boride, and silicide interdendrite phases by the stretching, necking, and plastic elongation of the nickel-phase dendrites in the wake of a crack tip that is propagating through the continuous brittle matrix” [7]. In Fig. 4 arrows indicates the stretching, necking, and plastic elongation of the nickel-phase dendrites and the rupture of the precipitated carbides. A proof of this conclusion is the fact that cracking was substantially reduced in the T40 samples and was absent in all of the processed T30 specimens as illustrated in Fig 4.

### 3.2. Wear

The wear rate for each coating gave values for T30 and T40 of  $0.0176 \cdot 10^{-9} \text{ KgN}^{-1}\text{m}^{-1}$  and  $0.0242 \cdot 10^{-9} \text{ KgN}^{-1}\text{m}^{-1}$  which were lower than that obtained for T60,  $0.0375 \cdot 10^{-9} \text{ KgN}^{-1}\text{m}^{-1}$ . The wear rate of the counterbodies of T30 and T40 were also similar ( $0.00142 \cdot 10^{-9} \text{ KgN}^{-1}\text{m}^{-1}$ ) and one order of magnitude lower than that obtained for T60 ( $0.0233 \cdot 10^{-9} \text{ KgN}^{-1}\text{m}^{-1}$ ). The matrix of T60 has the highest hardness, which explains why its counterbody has the higher wear rate. However, as it is also less ductile, it would justify the T60 having a higher wear rate: inspection of worn coatings suggested a wear mechanism of adhesive wear for T30 and T40 and microcutting and microploughing for T60. This agrees with wear theories indicating a wear mechanism transition depending on the properties of the worn material [7], where predominant abrasive wear changes to predominant adhesive wear. In the coatings of T60, the interdendritic eutectic predominates over the nickel-phase dendrites and in the coatings of T30 nickel-phase dendrites are the predominant phase. The nickel-phase dendrites are very ductile and prone to adhesive wear. In Fig. 5 we have a confocal microscopy image of the wear track on T60, T40s and T30 coatings. We can see, in the wear track on the T60 coatings, the comet tails that are typical in the abrasive wear mechanism. In the wear tracks on the T30 coating we can see the phenomenon of ductile layering, the ductile asperities of the T30 matrix are easily deformed which result in flat extended wear particles. The T40 coating show a mixed wear mechanism of adhesive and abrasive wear.

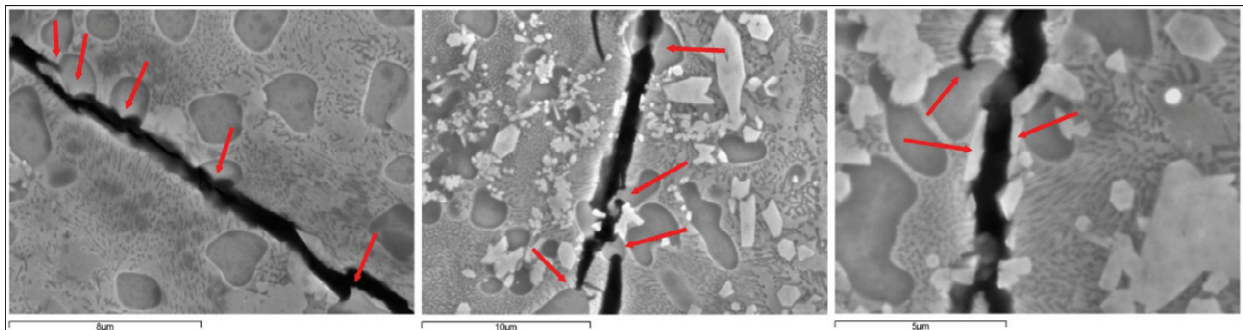


Figure 4. Crack propagation in the T60 layer. Arrows indicates the stretching, necking, and plastic elongation of the nickel-phase dendrites and the rupture of the precipitated carbides.

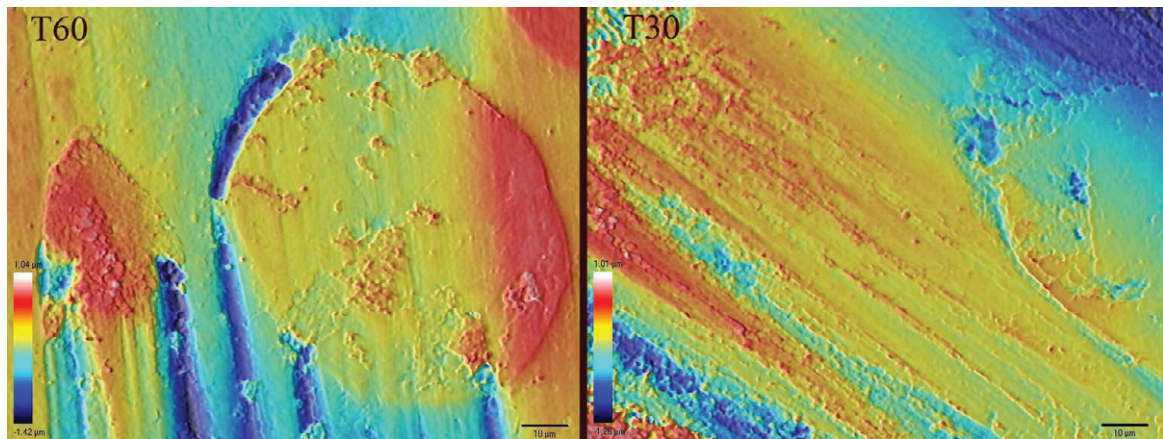


Figure 5. Confocal microscopy image of the wear track on T60 and T30 coatings.

#### 4. Conclusions

NiCr-WC MMC layers using commercial premixed alloy powder were deposited on a low carbon steel by laser cladding. Reinforcement tungsten particles consisted in spheroidal fused tungsten carbides. Three NiCr alloys acting as metallic matrices were tested which differed in their Cr content. Through careful parameter selection pore free layers with minimal dilution and good metallurgical bonding with the substrate were obtained. EDX analysis inspection and microhardness measurements yielded a reduced presence of tungsten on the matrix with compositions and hardness close to the nominal values. Cracking of the deposited coatings was related to the chromium content of the NiCr matrix. For composition with Cr(wt%) roughly below 8% no cracks were observed in any of the deposited samples. Wear studies, indicate that the loss in matrix hardness by reducing the Cr content does not imply a loss in the wear rate of the resulting coating.

#### Acknowledgements

This work has been done under the financial support of Xunta de Galicia, project reference 08DPI024CT, Programa de Diseño y Producción Industrial.

#### References

- [1] W.M. Steen, Laser Material Processing (3rd ed.), Springer-Verlag, London-Berlin Heidelberg (2003).
- [2] Van Acker, K., Vanhoyweghen D., Persoons R., Vangrunderbeek J.: Influence of tungsten carbide particle size and distribution on the wear resistance of laser clad WC/Ni coatings. In: *Wear*, 258, (2005), pp.194-204.
- [3] Huang S.W., Samandi M., Brandt M.: Abrasive wear performance and microstructure of laser clad WC/Ni layers. In: *Wear*, 256, (2004), pp.1095-1105.
- [4] Amado, J. M., Tobar, M.J., Alvarez, J.C., Lamas, J., Yáñez, A. In: *Appl. Surf. Sci.*, 10, (2009), pp.5553-5556.
- [5] ASM Speciality Handbook: Nickel, Cobalt and Their alloys. Ed. J.R. Davis. 2000.
- [6] R.C.Gassmann. Laser cladding with (WCW2C)/CoCrC and (WCW2C)/NiBSi composites for enhanced abrasive wear performance. In: *Mater. Sci. Technol.*, 12, (1996), p.691-696.
- [7] Cockeram, B. The fracture toughness and toughening mechanisms of nickel-base wear materials. In: *Metall. Mater. Trans. A*, 2002, 33, pp. 33-56.
- [8] Karl-Heinz Zum Gahr. *Microstructure and wear of materials*. Elsevier. 1987.